

INVESTIGATION OF STRUCTURE FORMATION OF SHS PRODUCTS IN MODEL EXPERIMENTS

V. A. Shugaev, A. S. Rogachev,
and A. G. Merzhanov

UDC 548.737

A method is developed that enables one to model extreme temperature regimes for heterogeneous reactions, to study the mechanisms of structure formation at a microscopic level, and to perform micrography of the process of interaction.

The key problem in producing SHS materials is the formation of a product with the required phase composition and structure in a combustion wave [1]. In order to purposefully regulate structure formation in synthesis of materials, it is necessary to know the mechanisms of formation of the structure and phase composition under SHS conditions. Several experimental procedures for the investigation of these mechanisms are presently known. Starting from the early works on SHS, hardening of intermediate products in the process of combustion by immersing a burning specimen in liquefied argon has been used to advantage [2].

Improving the hardening methods (hardening in a wedge-like cut of a copper massive block and cooling by a water jet) made it possible to bring the cooling rate to several thousands of degrees per second [3-5]. As a result of these works, the basic features of structure formation in the systems Ti-C, Ti-B, Ti-N and others were established. The formation of a crystal structure and a phase composition was investigated directly in the process of combustion using dynamic x-ray phase analysis [6-8].

The analysis of structure formation in a combustion wave is made difficult by the fact that the reacting heterogeneous mixture has itself a complex spatial structure with random contacts between particles. Therefore to study fine mechanisms of structure formation it is more convenient to deal with the interaction of a single powder particle. Thus, in [9] a particle of one reagent was heated by an electron beam in vacuum on a substrate of the other reagent. The results of the interaction were recorded with the aid of an electron microscope. The drawback of this procedure is the impossibility of accurately controlling the temperature of the reacting mixture. The work [10] using the electrothermographic method investigated the interaction of metal wires with a soot layer covering them. It determined the ignition temperature for such a layered system and obtained the effect of capillary spreading of metal. The work [11] proposed the development of the previous method. The authors utilized a computerized electrothermograph, which made it possible to faithfully reproduce the prescribed temperature regime (for example, the combustion wave thermogram). The model systems were also metal threads covered with a layer of the second reagent. Such a geometry is far from the real structure of a heterogeneous mixture and hence prevents many important features of the first steps of structure formation (for example, spreading) from being studied. Thus, the problem of developing the procedure of model experiments, which enable one to correctly extend the results to processes occurring in the SHS wave, remains topical.

The aim of the present work was to experimentally simulate the processes of structure formation for SHS products, taking maximum account of both the structure of simulated systems and the conditions in the combustion wave. The potentialities of the procedure are illustrated by three practically important systems of SHS. When studying the process of structure formation, use is made of an integrated approach, which includes high-temperature micrography, hardening of model systems and real mixtures, and application of currently available physical methods for investigating hardened structures.

Institute of Structural Macrokinetics, Russian Academy of Sciences, Chernogolovka. Translated from *Inzhenerno-fizicheskii Zhurnal*, Vol. 64, No.4, pp. 463-468, April, 1993. Original article submitted March 12, 1992.

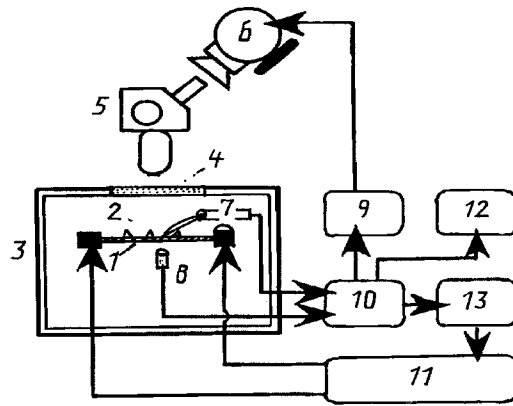


Fig. 1. Diagram of the experimental plant: 1) foil; 2) powder; 3) vacuum chamber; 4) glass window; 5) high-temperature microscope; 6) high-speed cine camera; 7) thermocouple; 8) photodiode; 9) control block for starting the cine camera; 10) temperature control block; 11) electric heater; 12) recording block; 13) heater control block.

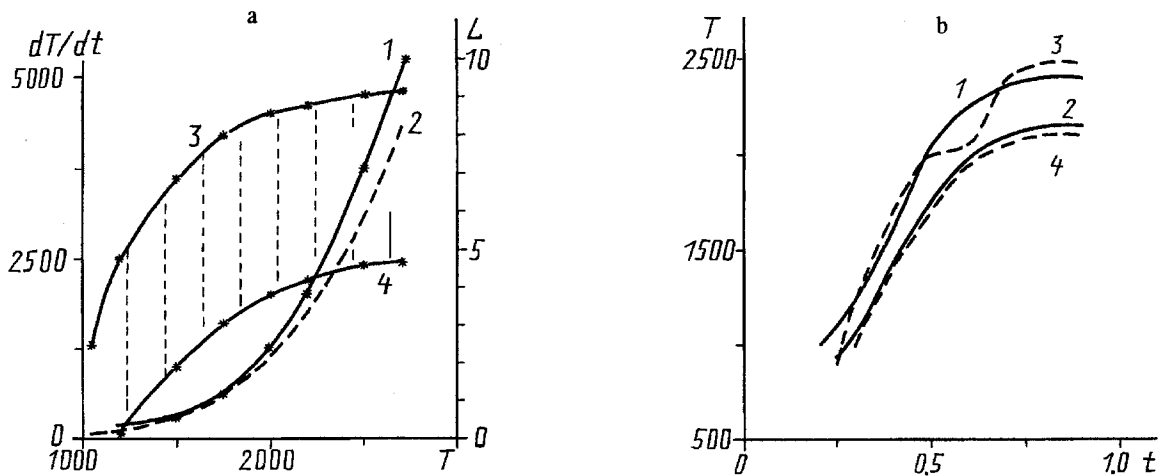


Fig. 2. Thermal conditions realized in the experiments in heating the foil of niobium: b) thermogram of heating of the niobium foil in the experiments (1, 2) as compared to the data [16, 17] on the temperature growth in the combustion wave front of the systems Nb-B (3) and Nb-2B (4); a) cooling rate in the middle of the niobium foil at different temperatures of the specimen (1 - experiment; 2 - calculation) and the size of the isothermal section in the middle of the foil as a function of temperature for foils of different length (3 - L=10, 4 - 5 cm). dT/dt , K/sec; T, K; L, cm; t, sec.

Experimental Procedure. Figure 1 shows a diagram of an experimental plant assembled on the basis of a vacuum universal post VUP-5.

To study the interaction in binary systems, use was made of a foil heated by electric current and a powder of the second reagent applied to the foil surface, or a mixture of two reacting powders on the surface of the heated foil. The substrate temperature was varied in the interval 900-3000 K; the holding time at the experimental temperature was from 0.1 to 120 sec. Foils Ni, Ti, Nb, Mo, Ta, W, and C in the form of a ribbon or a U-shaped boat 50-200 μm thick, 5-10 cm long, and 1-5 mm wide served as substrates. The foils were pre-polished with diamond pastes to remove broaching stripes, were cleaned in alcohol by an ultrasonic disperser, and subsequently were subjected to ionic etching in argon plasma and annealing and recrystallization in vacuum (10^{-5} mm Hg) at a temperature from 1300 to 3000 K. Narrow fractions (from 1 to 150 μm) of the following elements: Al, Ni, Ti, Si, and

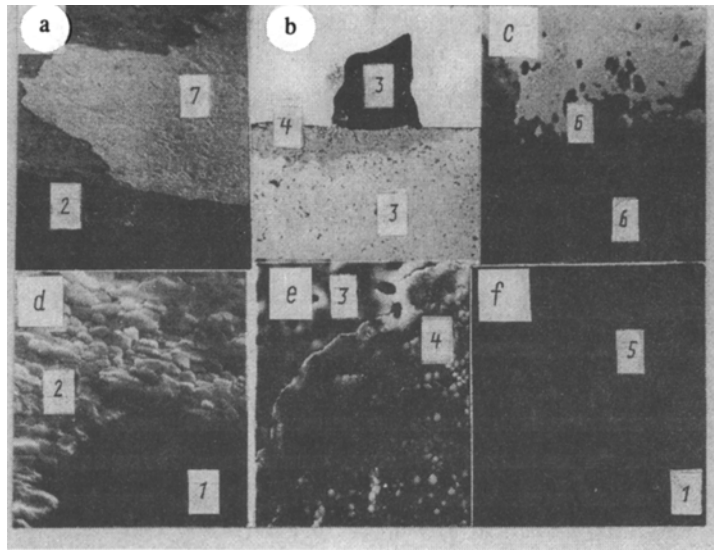


Fig. 3. Microphotographs of the structure of the yielded products: a-c) breaks and joints; d-f) structure of the yielded product; the system Ti-C, $T = 2000$ K, $t = 0.1$ sec: a) $\times 200$, SEI; d) $\times 3500$, SEI; the system Nb-B, $T = 2400$ K, $t = 0.1$ sec: b) $\times 700$, BEI; e) $\times 4700$, SEI; the system Ni-Al, $T = 1300$ K, $t = 0.2$ sec: c) $\times 1200$, BEI; f) $\times 4000$, SEI; 1) graphite substrate; 2) layer of TiC; 3) niobium; 4) product of NbB_2 ; 5) boron; 6) nickel foil; 7) layer of Al_3Ni_2 .

B served as powders. A modified alternating-current source (power 15 kW) incorporated in the VUP-5 served as a heater. Heating of the specimens was performed in two regimes:

- 1) the constant-power regime with simultaneous recording of the substrate temperature;
- 2) the constant-temperature regime realized owing to the introduced temperature feedback block (control with the aid of a thermocouple or by a luminous flux, as in [10]).

Micrography with the aid of a high-speed camera was performed during the experiment. The foil temperature in the experiment was recorded by a photodiode (the time constant was 10^{-5} sec) located on the foil side, where no reaction took place, and pre-calibrated using a tungsten-rhenium 50-micrometer thermocouple welded to the foil. On this surface there was no change in the emissive power of the foil in the reaction. This method is correct when there is no temperature distribution across the foil thickness ($Bi \ll 1$). Since heat transfer (ignoring heat removal to the electric contacts, i.e., if the foil length is large) occurs only at the expense of radiation in vacuum, then using the

values of $\lambda(T)$ from [12] and those of $\varepsilon(T)$ from [13] and taking into account that $\alpha_{rad} = \frac{\varepsilon(T)\sigma(T^4 - T_0^4)}{T - T_0}$ one can

calculate $Bi = \alpha_{rad}d/\lambda$. For the investigated materials and foils 50-200 μm thick in the temperature interval 1000-3000 K the calculated values lie within 10^{-3} - 10^{-4} . Thus, the temperature distribution across the foil thickness can be ignored. The calibration of the photosensor was performed on the 50-micrometer tungsten-rhenium thermocouple.

The work [14] considered in detail methodical errors arising in measuring the foil temperature by contact methods. The systematic errors of measuring the foil temperature by a thermocouple are due to removal of heat via cylindrical thermoelectrodes. Using the recommendations given in this work we calculated the error of measuring the temperature, taking into account the thermophysical properties of the material of the foil and the thermoelectrodes and the relation of their geometric dimensions. Thus, for example, the systematic errors in measuring the temperature of a 100-micrometer niobium foil with 50- and 100-micrometer tungsten-rhenium thermocouples are respectively 100 and 200 $^\circ$ at the melting temperature of niobium. By the same procedure one can make an estimate of the temperature of particles on the foil surface, assuming them to be infinite bars with a diameter equal to the particle diameter. These estimates show that for particles of size 100 m the difference in temperature does not exceed 50 $^\circ$. The calibration of the photosensor was performed under stationary conditions by a method of two thermocouples proposed in [15]. The true temperature of the foil was determined by the formula

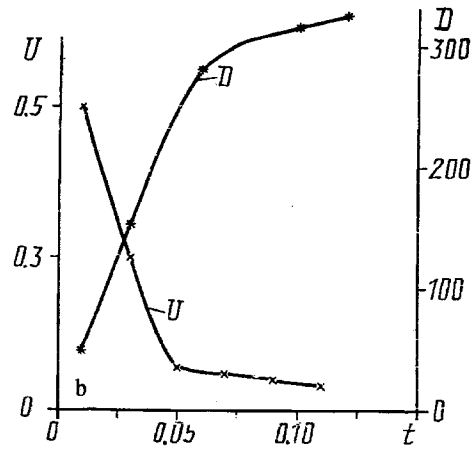
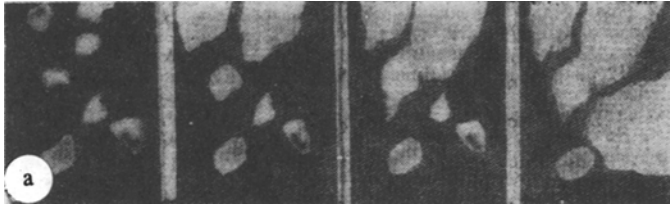


Fig. 4. Results of cinemicrography of the process of interaction between a boron particle and a niobium substrate at temperature 2400 K: a) photographs of the process of reaction spreading, the time interval between the presented pictures is 0.1 sec, x50; b) time dependence of the spread zone size D and the spreading rate U for a single boron particle. U , cm/sec; D , μm .

$$T = T_1 (1 - K_c) / (1 - K_c T_1 / T_2),$$

where T_1 and T_2 are the readings of thermocouples of different diameter; K_c is the correction factor, found from the results of the calibration experiment at the known temperature (for example, at the foil melting temperature or at the melting temperature of powders on the foil surface). Subsequently we constructed a plot: the foil temperature readings of the 50-micrometer thermocouple, and the brightness temperature recorded by the photodiode was set into correspondence with the true temperature of the foil. Figure 2a gives results on the hardening rate in the middle of the foil and the size of the isothermal section. The hardening rate for niobium foil in the interval 1800–2700 K lies within 2000–5000 deg/sec. The isothermal section increases in the middle of the foil with increasing temperature on account of a decreased contribution of heat transfer to the contacts.

Figure 2b shows the thermogram of heating of niobium foil as compared to the temperature growth in the combustion wave front [16, 17]. It is evident that the heating rate for the foil is comparable with the rate of temperature growth in the combustion wave front.

Experimental Results. The present work gives the results of investigation for three systems: Ti-C, Nb-B, and Al-Ni. Niobium and nickel 100-micrometer foils and a 70-micrometer carbon plate placed on a 50-micrometer tungsten foil served as heated substrates. Fractions from 20 to 150 μm of titanium, boron, and aluminum powders served as powders applied to the substrate. The choice of these systems is conditioned by the practical importance of the products, the presence of temperature profiles of the combustion wave, and the fact that in these systems it is possible to observe the interaction of a molten nonmetal with a hard metal (Nb-B), a molten metal with an unmelted nonmetal (Ti-C), and a molten metal with an unmelted metal (Al-Ni). Prior investigations of the interaction below the melting temperature of a lower-melting reagent have shown that the interaction occurs in the regime of reaction diffusion with large interaction times (>30 sec), yielding crystal-shaped products.

Figure 3 gives photographs of specimens produced with $T > T_0$ of melting of a low-melting reagent. It is evident that in all cases the product has a round cut, the ratio between the diameter of the spread stain and the thickness of the yielded product being different for all the three cases. This ratio (δ/D) is minimal for the system Ti-C and maximal for the system Ni-Al. The thickness of the product layer for the system Ti-C is equal to 1 μm , Nb-B to 10 μm , and Ni-Al to $\sim 30.0 \mu\text{m}$. In the latter case there is no spreading of Al over Ni, yet the substrate is "eaten through." Investigation of the dependence of the diameter of the initial boron powder on the diameter of the spread stain of the product in the system Nb-B made it possible to describe the results by the formula $D = bD_0^{1.5}$, where D is the size of the product stain; D_0 is the boron particle size; $b = 0.36 \mu\text{m}^{-0.5}$. This suggests the constant thickness of the layer

NbB₂, which is confirmed by the results of metallographic analysis. The distribution of the product grain sizes in the systems Ti-C and Nb-B over the stain diameter depends weakly on the distance from the stain edge; they increase from 0.5 to 2 μm in proportion to approach to the center. There is also a weak correlation between the size of the product grain in the center of the stain and the stain size (mass of the initial grain of powder), this dependence having saturation for sizes of the initial particle larger than 70-100 μm . Data of x-ray phase analysis and x-ray microanalysis made it possible to establish that in the first stage of the interaction in melting (spreading stage $t \sim 0.1$ sec) a single-phase product TiC forms in the system Ti-C, NbB₂ in the system Nb-B, and Al₃Ni₂ in the system Ni-Al. On further holding at a temperature (>30 sec) equal to T_m , formation of products depleted of the low-melting component takes place through reaction diffusion of this component into the nonreacted initial substrate, yielding products (NbB, Ni₃Al) that have a crystal cut. And in the system Ti-C there is no change in the composition of the formed product because titanium does not dissolve in a graphite substrate.

Figure 4a gives photographs of cinemicrography for the process of spreading of single boron particles over a niobium foil. On the basis of these results the diameter of the spread stain vs time is plotted (Fig. 4b), which enables us to determine the spreading rate, equal to 0.05-0.5 cm/sec. In Fig. 4a we can see a lighter region in the spreading zone, which suggests an elevated temperature in the zone of interaction of the melt with the substrate. Investigating the combustion temperature for a mixture of Nb and B powders on a tungsten substrate by a local optical method enabled us to determine this temperature, equal to 2800 K. By considering the experimental results one can draw the following conclusions.

1. An intense interaction in the systems with melting begins when T_m of a low-melting reagent is attained.
2. Spreading of the reagent in the time 0.1 sec (or eutectic) occurs, yielding the product, which prevents interaction of the melt and the substrate. (In the case of interaction between Al and Ni this temperature is higher and is equal to 1200-1500 K because the oxide film of Al prevents spreading.)
3. The structure of the product is globular.
4. Further interaction occurs in the regime of reaction diffusion.

Comparing the structure of the primary product with that of the product yielded by hardening the front in a copper wedge has shown its identity; the boundaries of the spreading zone were revealed. At the same time the model experiments enable us under rigidly controlled conditions to more completely and in greater detail study problems of structure formation.

Conclusions. Investigation of the interaction of powders with foil under controlled conditions makes it possible to determine the temperature of the onset of intensive interaction and the rate of spreading of the melt over the substrate, to establish the composition and structure of the primary product, and to investigate the dynamics of phase formation.

REFERENCES

1. A. G. Merzhanov, Self-Propagating High-Temperature Synthesis, Twenty Years of Search and Findings, I-CP-88P, ACerS Bull., 67, No. 9, p. 1505 (1988).
2. A. G. Merzhanov, I. P. Borovinskaya, and Yu. E. Volodin, Dokl. Akad. Nauk SSSR, 206, No. 4, 905-908 (1972).
3. A. S. Rogachev, A. S. Mukas'yan, and A. G. Merzhanov, Dokl. Akad. Nauk SSSR, 297, No. 6, 1425-1428 (1987).
4. A. G. Merzhanov and A. S. Rogachev, "Structural macrokinetics of SHS processes," Pure and Applied Chemistry (1992).
5. A. S. Mukas'yan, E. A. Bukreev, B. M. Khusid, et al., "Structural macrokinetics of the interaction of titanium with nitrogen in the combustion regime" [in Russian], Preprint, A. V. Luikov ITMO, Minsk (1991).
6. V. V. Boldyrev, V. V. Aleksandrov, M. A. Korchagin, et al., Dokl. Akad. Nauk SSSR, 259, No. 5, 1127-1129 (1981).
7. J. B. Holt, J. Vong, E. Larson, et al., Proceedings of the First US-Japanese Workshop on Combustion Synthesis, Tokyo (1990), pp. 107-113.
8. A. G. Merzhanov, I. P. Borovinskaya, V. I. Ponomarev, et al., "Dynamic radiography of transient processes", Dokl. RAN, 328, No. 1, 72-74 (1993).
9. M. A. Korchagin and V. V. Aleksandrov, Fiz. Goreniya Vzryva, No. 1, 72-79 (1981).

10. S. G. Vadchenko, Yu. M. Grigor'ev, and A. G. Merzhanov, *Fiz. Goreniya Vzryva*, No. 12, 676-682 (1976).
11. S. L. Kharatyan, G. A. Voskerchan, and A. G. Merzhanov, *Dokl. Akad. Nauk SSSR*, 316, No. 2, 415-419 (1991).
12. V. E. Zinov'ev, *Thermophysical Properties of Metals at High Temperatures: Handbook* [in Russian], Moscow (1989).
13. A. E. Sheindlin (ed.), *Radiative Properties of Solid Materials: Handbook* [in Russian], Moscow (1974).
14. N. A. Yaryshev, *Izv. Vyssh. Uchebn. Zaved., Priborostroenie*, 6, No. 1, 134-141 (1963).
15. N. A. Yaryshev, *Theoretical Foundations of Measuring Nonstationary Temperatures* [in Russian], Leningrad (1967).
16. A. A. Zenin, A. G. Merzhanov, and G. A. Nersisyan, *Dokl. Akad. Nauk SSSR*, 250, No. 4, 880-884 (1980).
17. A. A. Zenin and G. A. Nersisyan, *Khim. Fizika*, No. 3, 411-418 (1982).